Journal of Molecular Spectroscopy **202,** 107–115 (2000)
doi:10.1006/jmsp.2000.8104, available online at http://www.idealibrary.com on IDEAL®

Modern Millimeter-Wave Resonator Spectroscopy of Broad Lines

A. F. Krupnov, M. Yu. Tretyakov, V. V. Parshin, V. N. Shanin, and S. E. Myasnikova

Applied Physics Institute of RAS, 46 Uljanova Street, 603600 Nizhnii Novgorod GSP-120, Russia

Received January 18, 2000; in revised form March 1, 2000

Broad line millimeter-wave resonator spectroscopy is shown to have high sensitivity and fast and broad frequency scanning possibilities. Methods of absolute measurement of separate line, sample, and resonator losses are demonstrated and discussed. The primary radiation source (BWO) frequency is controlled digitally with minimal steps of a few hertz and switching time of 200 ns. An open Fabry–Perot resonator with a quality factor of ~600 000 is used. A resonance-width measurement accuracy of 20 Hz is reached which corresponds to an absorption coefficient sensitivity limit of $\sim 4 \times 10^{-9}$ cm^{-1} (0.0018 dB/km). *In situ* open atmosphere spectra records at 44–98 and 113–200 GHz are obtained in one experiment each. Lines of atmospheric oxygen and atmospheric water are observed. The water line at 183 GHz fits the Van Vleck–Weisskopf shape up to 20 half-widths from the line center within experimental accuracy. The dry-air broadening parameter for this water line is defined as 3.985(40) MHz/Torr. Atmosphere absorption in a 140-GHz window is measured. Results from other authors are compared. Possible applications of the modern broad line millimeter-wave resonator spectroscopy including real-time monitoring of open-air atmosphere and technological processes and measurement of absorption in thin dielectric films and conducting surfaces and metals are discussed.

Key Words: resonator spectroscopy; precise millimeter-wave measurements; digital fast frequency scan; atmosphere absorption lines.

I. INTRODUCTION

Resonator or cavity spectroscopy is one of the main directions of progress of microwave spectroscopy (*1*). Resonator spectrometers were divided by Townes into two main classes in the 1950s depending on the absorption linewidth in relation to the cavity resonance width: (i) the line is narrower than the cavity resonance and (ii) the line is much broader. The first case includes high-resolution spectroscopy but the second one covers high-pressure-broadened and atmospheric spectral lines as well as absolute measurement of radiation absorption at one fixed frequency. The first class was then extensively developed and the number of spectrometers reached an absorption-coefficient sensitivity close to the theoretical limit. The following examples can be pointed out: submillimeter-wave radio-acoustical spectrometry with a quasi-optical Fabry–Perot cavity gas cell (*2*), where the resonator served as a high-quality multipass cell, increasing the sensitivity of the device up to 3×10^{-11} cm^{-1}; millimeter-wave orotron-based spectrometry (*3*), where the gas sample was placed inside the orotron's resonator so the gas absorption was included into feedback of generated radiation by analogy with laser intracavity spectrometers (achieved sensitivity was about 3×10^{-10} cm^{-1}); millimeter-wave spectrometry with a highest quality Fabry–Perot cavity of which the resonance width was even narrower than a Doppler-broadened spectral line (*4*), which scanned the eigenfrequency of the resonator synchronously with the frequency of radiation source over the spectral line range to achieve a sensitivity of 3×10^{-10} cm^{-1}.

Our paper deals with spectrometers of the second class. They have probably not been pushed as intensely as the first ones; nevertheless as best examples the setup of Liebe *et al.* (*5*) was used for the study of millimeter-wave radiation absorption in the Earth's atmosphere, and the spectrometer described in the work (*6*) serving for 183-GHz water-line pressure-broadening investigations can be named. Absorption coefficient sensitivity in both of these apparatus was about 10^{-8} cm^{-1}. Although expressed in the same units, the sensitivity of this class device means minimal observable absorption or its variation in comparison with the absorption coefficient of the minimal observable spectral line (which is, in fact, also an observation of absorption variation over the line profile) in a first-class spectrometer.

Sample absorption measurement by this branch of resonator spectroscopy consists after all in comparison of the quality factors of the empty and loaded resonator. The resonator quality factor Q is defined as the ratio of the frequency of the resonance f_0 to the width of the resonance (FWHM) Δf. The sensitivity of resonator spectroscopy increases with an increase in the resonator quality factor and an increase in the resonance width measurement accuracy.

A combination of the Fabry–Perot resonator with $Q \sim$ 600 000 and fast precisely controlled and powerful enough broadband backward wave oscillator (BWO)-based synthesized radiation source permitted us to get the broadest spectra ever observed by means of broad line resonator spectroscopy and to obtain an absorption coefficient sensitivity significantly exceeding that previously known. The achieved sensitivity allowed us to develop methods of separation of (i) resonance

0022-2852/00 $35.00

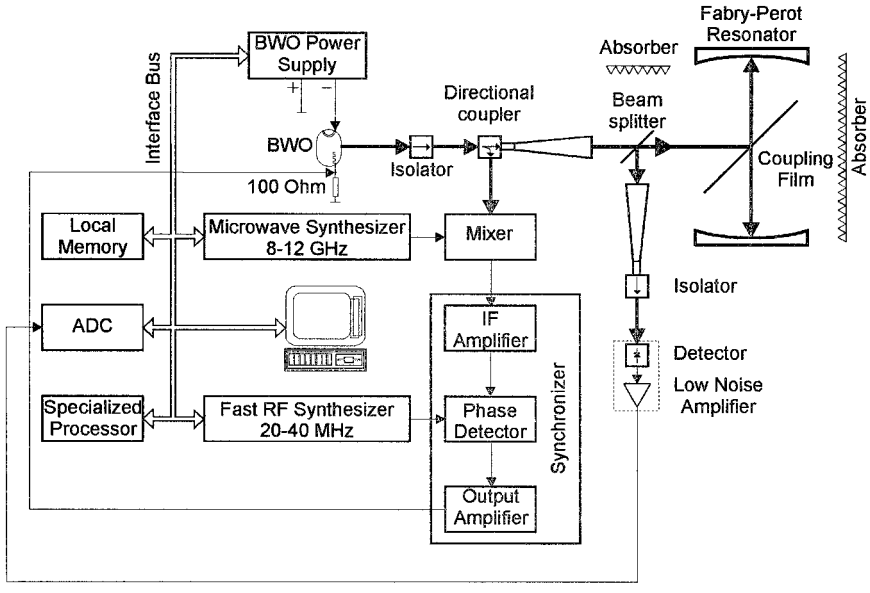

FIG. 1. Block diagram of the experimental setup of the resonator millimeter-wave spectrometer. Radiation source is BWO, the frequency of which is controlled by PLL including slow MW and fast RF reference synthesizers. The sensor is a high Q Fabry–Perot resonator. Detector of the radiation passed through the resonator is Schottky diode. Control of synthesizers, data acquisition, and processing are performed by computer.

absorption in spectral lines, (ii) nonresonance absorption in a sample filling the resonator, and (iii) the resonator losses, all three without removing the sample from the resonator.

Our first communications concerning development of this class of spectrometers were in (*7*, *8*).

The general aim of the present work is to approach by broad line resonator spectroscopy the sensitivity, convenience, absolute absorption measurement, and broad scanning possibilities of common microwave spectroscopy, but at much higher pressures, in a real-time regime, and in as high a frequency range as possible. This would permit us to extend the possibilities of microwave spectroscopy. In this paper we describe observation of the molecular spectra by microwave methods in open atmosphere *in situ.* Extension to atmospheric pressure and to open atmosphere gives a method of microwave monitoring of atmosphere (or other gas mixtures) constituents which is of scientific as well as of applied importance. Possibilities and perspectives of modern resonator microwave spectroscopy of broad lines as well as some new directions opened for studies and applications are discussed.

II. APPARATUS

The block diagram of the apparatus is presented in Fig. 1. The Fabry–Perot resonator used the fundamental $TEM(00q)$ mode, where q is the longitudinal mode number, i.e., the number of half-wavelengths between mirrors. The quality factor of a Fabry–Perot resonator having length 25–42 cm, spherical silver–plated mirrors 12 cm in diameter and 24 cm in curvature radius, coupled with source and detector by 6-μm Teflon film placed at 45° to the resonator axis, was defined by unavoidable reflection losses (silver is the best reflecting material in the millimeter-wave range). The approach to the construction of high quality-factor Fabry–Perot resonators is outlined in (*7*), where contributions of various components of losses in a properly constructed resonator with high Q factor are analyzed.

There are several sources of radiation losses in the resonator. As is known, the width of the resonance can be written as

$$\Delta f = \frac{cP_{\text{total}}}{2\pi L}, \qquad [1]$$

where c is the velocity of light in a substance, L is the resonator length, and P_{total} are total relative losses of radiation energy during one traversal of the resonator. The length L is defined in our case as

$$L = \frac{\lambda}{2}\left(q + \frac{1}{\pi}\arccos\left(1 - \frac{L}{R}\right) - \frac{\lambda}{4\pi^2 R}\right), \qquad [2]$$

where λ is the wavelength in the substance, R is the mirrors' radius of curvature, and q is the number of half-wavelengths between mirrors (*9*).

Total losses in the Fabry–Perot cavity P_{total} consist of

$$P_{\text{total}} = P_{\text{reflection}} + P_{\text{coupling}} + P_{\text{diffraction}} + P_{\text{atmosphere}} \qquad [3]$$

and one needs some additional procedure to separate the losses to be measured. Expressions for all the losses are known with more or less accuracy: losses in the atmosphere filling the

resonator can be calculated using the program described in (*10*) and its updates (*5, 11*); diffraction losses can be calculated as a fraction of total energy accumulated inside the resonator which is cut by the resonator mirrors' aperture and can be done much smaller than all other losses; coupling losses can be calculated from (*12*) and coupling film parameters; reflection losses can be calculated from dc conductivity of bulk silver using expressions given, e.g., in (*13*).[1]

The synthesized frequency radiation source employ a backward wave oscillator (BWO) (*15*) which was stabilized by a phase lock-in loop (PLL) with the use in this case of two reference synthesizers: one microwave (MW) synthesizer (8–12 GHz) defining the central frequency of the BWO as described in (*16*), and one fast radiofrequency (RF) synthesizer (20–40 MHz) for precision fast scanning of the BWO frequency around the chosen central frequency. The radiofrequency synthesizer provides frequency scanning without loss of the phase of oscillations (without phase jumps). Both synthesizers are computer-controlled. As a result, the BWO frequency was defined as

$$f_{\mathrm{BWO}} = n \cdot f_{\mathrm{MW}} - 10 \cdot f_{\mathrm{RF}},$$

where n varied from 4 to 20, and a factor of 10 before f_{RF} appears because phase detection was done at 10 times the digitally divided intermediate frequency (IF), which was 350 MHz. The main source of error in measurement of the resonance width is the drift of the central frequency of resonance during the time of measurement. To minimize this error one has to measure the resonance curve as fast as physically possible. Response time of the resonator itself was $\tau \sim 1/\pi\Delta f \sim 2\ \mu$s. For precision measurement the observation time should be increased, say, 10 times, i.e., up to $\geq 20\ \mu$s. Microwave and millimeter-wave synthesizers commonly used for spectroscopy employ indirect frequency synthesis and so have ~(10–50) ms switching time, thus preventing fast scanning of the resonance curve. A fast direct radiofrequency synthesizer with switching time ~200 ns and time between switching 58 μs was used in this work as a source of a reference signal for the phase detector in the lock-in loop. Thus precision and fast scanning of the BWO radiation frequency within ~200 MHz around the central frequency defined by the microwave frequency synthesizer were attained. Scanning without loss of phase permits the physical limits of the resonance observation time to be approached and reduces the source phase noise. The passed-through resonator radiation was received then by a low-barrier Schottky diode detector. The precision frequency control, signal acquisition, and processing were done by computer, as is shown in Fig. 1 and will be explained below. Results of each scan were recorded and processed separately.

[1] We used silver conductivity value from (*14*). Calculated reflection losses differ from experimental ones less than by 10% (*7*). It is worth noting that values of conductivity themselves differ in different handbooks.

The automation system consisted of an IBM PC and a module containing an RF synthesizer and a data acquisition system. For minimization of ground-to-ground statics the module was connected with the PC by an optically coupled interface. The core of the module is a microprocessor with external memory. The RF synthesizer is based on direct digital synthesizer (DDS) microcircuit AD9850 (Analog Devices Inc.) and is able to generate a harmonic signal in the 20–40 MHz range with 0.03 Hz discreteness and without phase jumps at the switching. Data acquisition (digitizing of preamplified detector signal) is done by 12-digits ADC. Data are stored in data memory. A microprocessor controls the frequency of the synthesizer and synchronizes the data-acquisition process with the frequency steps. The microprocessor receives the parameters of the synthesizer frequency tuning from the PC: starting frequency, value of the frequency step, time of the next frequency step, number of points, frequency change law, and number of scans. Time between frequency changes was chosen for our purpose as 60 μs per point. The frequency was changed by a triangle law, meaning forward and backward scan. The maximum number of points per scan was 512. In each frequency point, the microprocessor collected data several times from the ADC, averaged the obtained results, and put the average into data memory. In such a way 32 of the 512 point triangle scans may be put into local memory. The number of scans which could be put into local memory increased proportionally by reducing the number of points per scan. So the process of registration of 32 scans with 512 points per scan took 0.98 s. After the ordered number of scans were recorded into local memory, the data were transferred to PC for further processing.

The processing consisted of a least-squares fitting of the results of each scan to Lorentzian with added linear[2] and constant terms representing effects of interference in the tract in the vicinity of resonance, level of noise on the detector, and bias voltage of amplifier:

$$F(f) = \frac{1}{(\Delta f/2)^2 + (f - f_0)^2} \cdot (A + B(f - f_0)) + C.$$

As a result of the fit, the width of the resonance Δf and the position of the center f_0 are obtained. Time necessary for the fitting of one scan depends primarily on the scan size and type of the PC processor. With a *P*120 processor and a 1024-point scan, this time varies from a split second to several seconds depending on the noise level. This time is defined for one single scan without using the results of the processing of the previous scan. The next scan processing time can be reduced to some tens of milliseconds by use of the previous scan processing result as initial fitting parameters. It is clear that some nonphysical time losses can be reduced, e.g., just by the change of the processor.

[2] Practice showed no necessity in quadratic term.

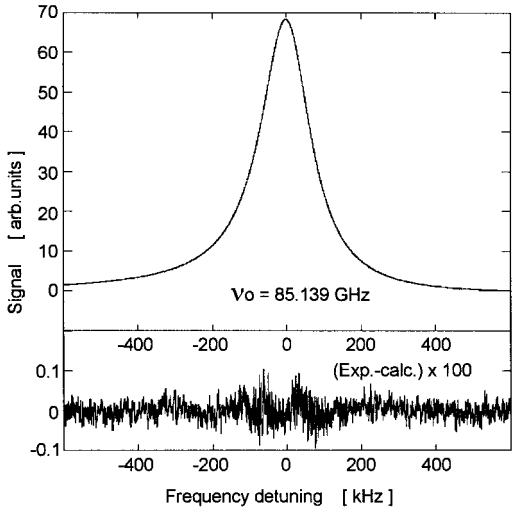

FIG. 2. Resonance curve of Fabry–Perot resonator record (500 centered scans). Residual of the fit to the Lorentzian curve multiplied by 100 is presented below. Measured width of the resonance (FWHM) at the frequency 85.139 GHz is equal to $\Delta f = 164\ 728(20)$ Hz.

III. EXPERIMENT

1. Measurement of Resonance Width

The basic procedure in resonator spectroscopy is to measure the width of the resonance. The experimentally observed resonant curve of the Fabry–Perot resonator at 85 GHz is presented in Fig. 2 as an example. The curve is a combination of 500 scans with a duration of 30 ms each, i.e., corresponding to the summary averaging time 15 s. Each fast scan was processed separately, then resonant curves were combined so their centers coincided, and so the averaged curve in Fig. 2 was obtained. The residual of the fit, shown in the lower part of the figure, indicates the adequacy of the fitting model. The increased noise on the line slopes corresponds to transformation of phase noise of radiation into amplitude noise. The width of the resonance (FWHM) was defined then as $\Delta f = 164\ 728(20)$ Hz. Of course, to obtain only the averaged value of the width one can just average the values of the widths obtained by processing each scan.

In Fig. 3 the inside story of obtaining the resonator width value by averaging single scan processing results is shown. The width is plotted vs number of averaged measurements: thin curves depict results of only forward (F) and only backward (B) frequency scans; the thick curve depicts the mean value of these two. Every point corresponds to 20 times the averaged value of width obtained from processing 30-ms duration single scans. Dependencies of curves in Fig. 3 show not only the effect of measurement accuracy increase with data accumulation, after 340 averaging the mean value of back and forth scans varies within 10 Hz, but also the significance of the fast frequency scan introduced by us for faster obtainment of the data as well as for lessening of the measurement errors arising from the resonance center frequency drift. Differences between width values measured with opposite directions of the scan reach 400 Hz due to the drift of the center frequency of the resonance during the time of the scan even for scans as fast as 30 ms. Change from slower scans used earlier (e.g., 10 s in (*7*)) to the 30-ms scan is in some sense equivalent to the change to modulation method (with 30-Hz modulation frequency) leaving behind for the most part a flicker-type of drifts and perturbations.

The sensitivity in the terms of the absorption coefficient defined from 20-Hz resonance width measurement accuracy constitutes $\sim 4 \times 10^{-9}$ cm^{-1} (or 1.8×10^{-3} dB/km). It does not differ very much from the sensitivity of common microwave spectrometers.

2. Broadband Resonator Spectroscopy

Fast broadband frequency scanning by the microwave Fabry–Perot resonator spectrometer of the class concerned can be achieved most conveniently without mechanical tuning of the resonator by just jumping the frequency of synthesizer from one longitudinal mode characterized by the index q to its neighbor $q \pm 1, 2, 3, \ldots$ depending on frequency increase or decrease. In our Fabry–Perot resonator the distances between two consecutive longitudinal modes constitute about 0.5 GHz, which means that inside a waveguide band on the order of 50–100 GHz bandwidth one obtains about 100–200 frequency points at which measurements can be made without mechanical tuning. Such a number of experimental points is good enough for obtaining a good representation of the spectrum considering width of the atmospheric lines. Of course, scanning slower with smaller steps using mechanical Fabry–Perot tuning is also possible. There is also a way to increase the resonator length, thus making the spectrum of modes more dense; but this has its limitations.

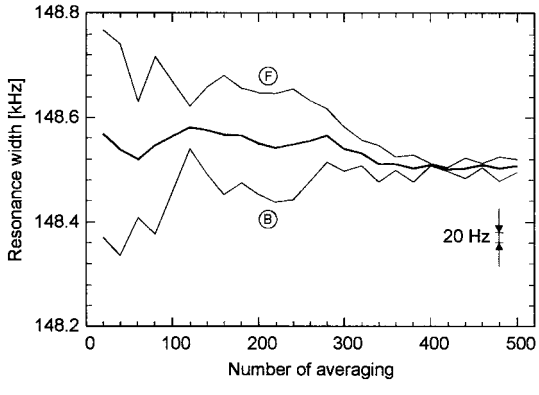

FIG. 3. Convergence of measured width of the resonance curve of Fabry–Perot resonator with the number of measurements. Results of forward (curve F) and backward (curve B) scans are presented separately, demonstrating existence of the fast drifts of the center resonance frequency even at scan times as short as 30 ms. Average of back and forth scans is shown (medium curve).

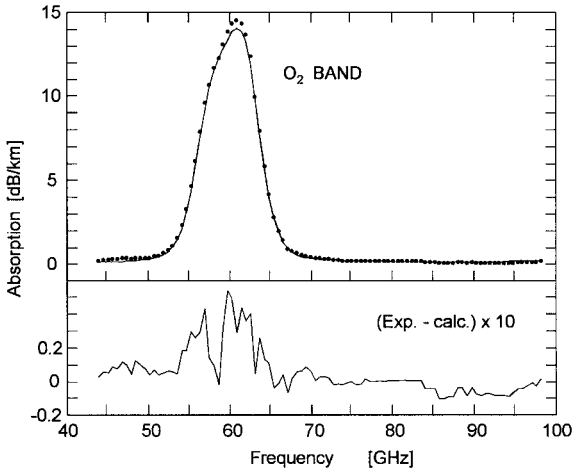

FIG. 4. The experimental spectrum of atmospheric air in 44–98 GHz frequency range including oxygen absorption band around 60 GHz compared with calculations (*11*). Residual multiplied by 10 is shown below.

(a) 44–98 GHz band. The first spectrum of the atmosphere studied by the described method was the oxygen band around 60 GHz. Preliminary studies were done in (*8*). Since then, the experimental setup was somewhat improved and a new program presenting the improved version (*11*) of the program described in (*10*) for calculating of atmosphere absorption in millimeter-wave band was kindly sent to us by Dr. P. W. Rosenkranz. So we decided to repeat these measurements.

The absorption spectrum of the laboratory atmosphere in the 44–98 GHz frequency range at atmospheric pressure is presented in Fig. 4. The spectrum includes an absorption band of atmospheric oxygen produced by magnetodipole transitions between fine structure rotational energy levels (see, e.g., (*17*)). Broad scanning in this experiment was produced as described above by jumping from one longitudinal mode to another. The circles in Fig. 4 represent experimental points (after subtraction of calculated resonator losses); the solid line is the calculation according to (*11*); the residual of the fit multiplied by 10 is presented at the bottom.

The spreading of experimental points in the regime of frequency scanning exceeds the value of the sensitivity defined from Fig. 2, obtained at one frequency point, because of numerous frequency dependencies in the apparatus. They mostly reflect interference in the radiation tract outside the resonator so the spreading can be considered as the device baseline and was reduced by placing isolators after the BWO and before the detector. Further reduction can be done by averaging ("smoothing") the variations having in mind that interference pattern frequency dependence is "faster" than any one of the aforementioned sources of the losses. The "most radical" way of reducing these baseline variations would be to reduce the coupling of the resonator with other parts of the setup, but this can be done only at the expense of the signal-to-noise ratio. Nevertheless, the sensitivity demonstrated by the scan in Fig. 4 exceeds the sensitivity of other known analogous apparatus.

Let us briefly discuss the obtained result. First of all it should be noted that the comparison of our O_2-band absorption experimental data presented in (*8*) with a spectrum calculated using the new program (*11*) gave beautiful results; we got a practically noise-looking residuum. But the new record again showed some divergence from the calculation which is clearly visible in the residual in Fig. 4. This leads us to the conclusion that the model accepted in (*10, 5, 11*) and widely used in practical calculations of absorption describes the 60-GHz band of atmospheric oxygen well to the $\sim \pm 2\%$ estimated calculation uncertainty done in (*5*), but more accurate modern experiment shows within the limits mentioned some regular deviations, the origin and conditions of the appearance of which is unknown at the moment. More detailed analysis of this falls out of the scope of the present paper and will be done elsewhere.

(b) 113–200 GHz band. The next absorption spectrum of laboratory atmosphere filling the Fabry–Perot resonator was taken in the 113–200 GHz frequency range also in the form of a set of resonance widths of consecutive longitudinal modes bearing information about total relative energy losses in the resonator in accordance with Eq. [1]. The calculated resonator losses have been subtracted from the experimentally determined total losses to obtain the atmospheric contribution, as in the previous experiment. The resulting dependence of atmosphere absorption vs frequency is presented in Fig. 5 by circles.

A line of oxygen at 118 750 MHz and a line of water at 183 310 MHz are visible in the record. Omitting the analysis of the weak oxygen line, we concentrated on the opportunity to investigate a relatively isolated single water line. Part of the

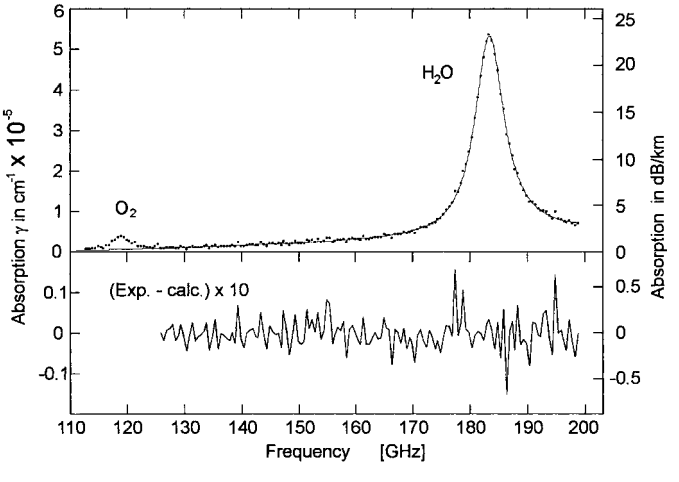

FIG. 5. Experimental 113–200 GHz scan of the spectrum of the real atmosphere inside Fabry–Perot resonator including atmosphere oxygen O_2 118 GHz and water H_2O 183 GHz absorption lines. Resonator losses are subtracted. Solid line, fitted to the experiment Van Vleck–Weisskopf profile with addition of constant, linear, and quadratic with frequency terms. Residual of the fit multiplied by 10 is presented below.

spectrum in Fig. 5 was fitted to the Van Vleck–Weisskopf lineshape given, e.g., in (*1*) with the addition of constant, linear, and quadratic frequency terms to account for possible inaccuracy of calculated resonator losses, nonresonance absorption of the filling resonator air, and the wings of strong higher frequency water lines. The resulting calculated function is shown in Fig. 5 by a solid line. Multiplied by 10, the residual of the fit in the range of fitting (125–200 GHz) is presented in the lower part of the figure.

Not considering at the moment the physical significance of another mentioned term obtained from the fit, let us analyze the spectral line obtained from the fit. An experimental line fitted the Van Vleck–Weisskopf shape over 20 half-widths from the center to the low-frequency side and six half-widths to the high-frequency side within experimental accuracy. A residual of the fit presented in Fig. 5 shows no systematic deviation from the theoretically calculated lineshape. So a really good-looking line was extracted from all the rest of the absorptions.

To study properties of the line obtained, it was of interest to compare values of integral absorption coefficients: one calculated from parameters of water and partial pressure of water in the atmosphere at the time of the experiment and another obtained experimentally from measured magnitude of absorption and the spectral line width obtained from the fit.

The integral absorption coefficient for relatively narrow lines ($\Delta\nu \ll \nu_0$, which corresponds to our case) was defined according to (*1*) as

$$\frac{8\pi^3 Nf}{3ckT}\,|\mu_{ij}|^2\nu_0^2 = \gamma(\nu_0)\cdot\Delta\nu,$$

where ν_0 is the line center frequency, $\gamma(\nu_0)$ is the absorption per unit length at the line center frequency (maximal absorption coefficient), $\Delta\nu$ is the line half-width, $|\mu_{ij}|$ is the matrix element of the molecule dipole moment for the given transition, T is the absolute temperature, k is the Boltzmann constant, c is the velocity of light, f is the fraction of the molecules in the lower two states of the transition, and N is the number of molecules per unit volume.

Integral absorption coefficient at $T = 292.8(1)\ K$, humidity 5.87(19) g/m^3, and pressure 759.1(5) mmHg (experimental atmosphere conditions) for the $3_{31} \leftarrow 2_{20}$ line of $H_2{}^{16}O$ molecule was calculated using expressions for f and $|\mu_{ij}|$ from (*1*) and values of rotational constants, dipole moment, and the transition lower level energy from the JPL data base[3] (*18*) as $1.513(50) \times 10^5$ cm^{-1} Hz. (The uncertainty is mostly defined by our air-humidity measurement error.)

On the other hand, from the fit of our experimental data, we found absorption at the center of the line $\gamma(\nu_0) = 4.932(22) \times 10^{-5}$ cm^{-1} and the line half-width $\Delta\nu = 3.131(21) \times 10^9$ Hz. Thus the experimental value of the integral absorption coefficient was obtained as $1.545(17) \times 10^5$ cm^{-1} Hz.

[3] http://spec.jpl.nasa.gov.

TABLE 1
Measured Air Broadening Parameters for 183-GHz Water Line

Absorption Path	Pressure Range	Temp. K	Broadening MHz/Torr	Ref.
Cell	10-250 mTorr	299	4.48 ± 0.11	(*21*)
Cell	5-400 μTorr	~300	3.52± 0.18	(*22*)
Field prop.	Atm.	≃284	4.14± 0.23	(*20*)
Field prop.	Atm.	300	4.04 ± 0.14	(*23*)
Resonator	Up to Atm.	≃300	4.04±0.3	(*24*)
Resonator	Atm.	292.8(1)	3.985 ± 0.04	this work

Comparison shows excellent coincidence (better than 2%) between measured (from the line profile obtained from the fit) and calculated (for a given quantity of water in atmosphere) values of integral intensity. This leads one to the conclusion that the line obtained from the fit of our experiment really corresponds to the line studied and correctly reproduces its main features. The procedure of extraction of the line parameters at atmospheric pressure was found in fact to be equivalent to the one in common microwave spectroscopy when the experimental profile is fitted, assuming the presence of unknown baseline.

The coincidence of calculated and measured integral intensities justifies the use of this convenient and precise method for measurement of integral intensity of spectral lines of other molecules at near-atmospheric pressures and also gives an absolute measure of air humidity just from parameters of the line obtained from the fit, which is important for the applications of the apparatus.

At the next step it was interesting to get from our experiment the water-line dry-air broadening parameter ($\Delta\nu_b^{\text{dry air}}$), which could be found from the formula

$$\Delta\nu = \Delta\nu_b^{\text{dry air}}\cdot(P_{\text{atm}} - P_{\text{water}}) + \Delta\nu_b^{\text{water}}\cdot P_{\text{water}},$$

where $\Delta\nu$ is the line half-width obtained from the observed profile fit; P_{atm} is the atmospheric pressure at the time of the experiment; P_{water} is the partial pressure of water vapor in the atmosphere, which can be calculated from measured air humidity; and $\Delta\nu_b^{\text{water}}$ is the broadening parameter of the line for pure water vapor, which was measured by us earlier (*19*) as 21.69(45) MHz/Torr.

The resulting value of air broadening is presented in Table 1 together with the values obtained by some other authors (*20–24*)[4] being somewhere in the middle of measured values and having better estimated accuracy.

[4] Compilation of air-broadening parameters for water lines can be found in the review (*20*).

Finally it should be noted that observation of the 113–200 GHz band containing a 118 GHz oxygen line and a 183 GHz water line, as far as we know, is the broadest spectrum record ever made by such a class of resonator spectroscopy in one experiment. Thus in scanning possibilities the modern resonator spectroscopy of broad lines also is not behind common microwave spectroscopy.

3. *Measurement of Gas Sample Absorption and Resonator Losses at One Fixed Frequency*

We describe here the method of separation of the resonator and sample losses. As far as we know, this variant of measurements was not used earlier because the accuracy of the resonance width measurements was less than ours.

The separation of the sample and resonator losses can be achieved in this case because each of three first terms in the expression for the total losses [3] remains constant at each fixed frequency (and can be denoted together as $P_{\text{resonator}}$), but the last term representing sample absorption depends on the distance between mirrors and can be rewritten in terms of the sample spectral absorption coefficient γ as

$$P_{\text{atmosphere}} = 1 - e^{-\gamma L}.$$

Considering the small optical depth case[5] ($\gamma L \ll 1$), the expression for resonator width as a function of the resonator length derived from [1] can be simplified to

$$\Delta f = \frac{c}{2\pi}\left(\frac{P_{\text{resonator}}}{L} + \gamma\right), \qquad [4]$$

which demonstrates that resonator losses and sample absorption can be considered as two independent parameters which can be unambiguously determined. There are two ways to do this: (i) to measure the function values at two different values of argument L and solve the system of two equations [4], or (ii) to experimentally obtain the function values over some range of arguments and fit the function parameters to get the best agreement. The first looks simpler and is preferable for practical applications of the settled apparatus but the second is more transparent for study of the method itself.

Figure 6 presents experimental dependence of resonance curve width vs resonator length at the same fixed resonance frequency. The resonator length is expressed through the number q of half-wavelengths between mirrors. Although only every third mode was studied, it can be seen from Fig. 6 that our high sensitivity permitted the accurate measurement of change in the width of the resonance when the length of the resonator was changed just by one-half wavelength, i.e., q by 1. The measurements were done by moving one of the resonator mirrors from one resonance to another, keeping the central frequency of scan constant. Circles represent experimental points; the solid line is the width function calculated in accordance with Eqs. [1]–[3] and is fitted to the experiment by variation of losses. The residual of the fit multiplied by 10 is also shown. Values of the resonator losses and a sample absorption coefficient (atmosphere absorption) determined from the fit are $P_{\text{resonator}} = 123.14(18) \times 10^{-5}$ relative losses of radiation energy during one traversal of the resonator and $\gamma = 9.904(53) \times 10^{-7}$ cm^{-1} (0.4301(27) dB/km) at the experimental frequency of 140 286 MHz.

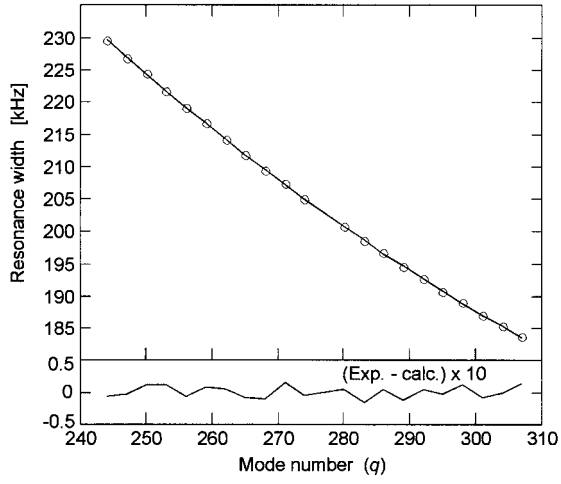

FIG. 6. The dependence of the resonance curve width vs the number of half-wavelengths between the mirrors q at one fixed frequency 140.286 GHz and result of its fitting to Eqs. [1]–[3]. Residual of the fit multiplied by 10 is shown at the lower part of the figure. Defined from the presented dependence atmospheric losses are equal to $9.904(53) \times 10^{-7}$ cm^{-1} (0.4301(27) dB/km).

Our experimental value of atmospheric absorption coincides well with the value 0.443 dB/km calculated by the semiempirical program (*11*) for the same atmospheric conditions. The obtained value of resonator losses was used for the correction of calculated losses in obtaining experimental dependence in Fig. 5.

In fact, the described method of atmospheric absorption and resonator loss measurement is a modification of the known method of path length variation often used in field propagation measurements, which became available in the present form with an increase in the accuracy of resonance width measurements. As it seems, this method is the best for this class of resonator spectroscopy because it can be used with a minimum of assumptions, so a minimum of systematic errors may be expected. Since the method does not require removal of the sample from the resonator, it has the advantage of smallest perturbation of the experimental conditions (no need to pump gas out, no need to wait for equilibrium to be restored, etc.).

At the completion of the experimental section it is worth noting that for investigations of atmosphere losses of radiation, the combined use of both methods described above permits the separate definition of absorption in the resonator (resonator

[5] It really corresponds to our case but is not principal since the accurate expression can be used in the fit as well.

losses), absorption in the line(s) (down to far wings), and "extra" or "nonresonance" absorption in the moist air. This study can be done very accurately because of the large reserve of sensitivity to help solve the long-studied problem of the origin of this nonresonance absorption by obtaining its quantitative spectrum.

IV. DISCUSSION

Coming to the discussion of more general properties of the broadband resonator microwave spectroscopy of broad lines it can be said that it successfully solves the problem which has limited maximal observable linewidth in the common microwave spectrometers. This is achieved in fact by change from amplitude measurements to frequency measurements, measurements of the widths of the "probe" resonance along the broad absorption line. Because width of the resonance is small in comparison with radiation tract interference variation periods, small changes of the amplitude in the vicinity of the resonance can be easily taken into account in the fitting procedure, and the amplitude plays only the role of a "scale factor," mostly defining the signal-to-noise ratio.[6] However, the price of getting rid of the interference problem is time. Instead of just one absorption-related amplitude measurement at one frequency, one has to make a number of measurements. The number should be large enough to restore the profile of the resonance with desired accuracy and to define the absorption-related width of the resonance. Now, when the described results permit saying that at the moment all the principal conditions for all automation of such spectrometers have been met, it is interesting to discuss the physical time limitations of this type of spectroscopy. Total time necessary to obtain a picture of the broad (covering waveguide band) spectrum by the aforementioned "nonmechanical" tuning is summed up as (i) obtaining one point on the resonance curve of high Q Fabry–Perot cavity, which demands by physical reasons more than 2 μs, say, $\simeq$20 μs; (ii) obtaining one resonance curve containing, say, 100 points in each of two (back and forth) scans, which then takes $\simeq$4 ms; (iii) obtaining of $\sim$100 pairs of such scans covering all waveguide band, which can be done in $\simeq$400 ms; (iv) processing, which may increase this time at most severalfold. Thus a full waveguide band spectrum picture can be obtained almost every second. As can be seen, this is a rather generous estimate and the observation time can be significantly reduced. Nevertheless, even this estimate means in our opinion practically a real-time regime of, e.g., atmospheric or technological processes monitoring. In the majority of practical cases one is interested not in the scanning of the whole waveguide band but rather in the monitoring of one peak (e.g., humidity monitoring); then the scanning time shortens and one can use time to average the signal and so improving the sensitivity.

As can be seen, the apparatus described in this paper was conceived as a broadly multipurpose device able to work automatically in real time in open air (or other gas). Our plans for further development of the apparatus include improvement of hardware (faster processor and interface, larger memory), realization of fully computerized frequency control (in our case BWO, but at the next stage a solid-state radiation source), and possibly change from a video detector to a superheterodyne receiver for further sensitivity increase.

Development of precision broadband resonator microwave spectroscopy of broad lines with the parameters described opens new possibilities in many fields of microwave spectroscopy and applications. In atmospheric studies new possibilities are open not only in lines studies, but also in the study of nonresonance absorption in the atmospheric transparency windows, in real-time dynamics of atmospheric process studies (atmospheric monitoring), in separation of the effects defining the atmosphere radiation absorption, and in the study of their dependencies on parameters. The high speed of absorption measurements, high sensitivity, and measurement by volume give wide possibilities for use of the method for humidity measurement: direct measurement of low humidities in higher atmosphere from flying apparatus; real-time monitoring of low humidities in technological processes such as optical fiber fabrication and work with dry materials, etc. Especially important to note is that sensitivity to low humidities can increase by further orders of magnitude by passing to much stronger water lines at higher frequencies.

Resonator spectroscopy in the variant described is universal in the sense of studied objects: increase of sensitivity, fast broadband scanning, etc., can be used for improvements, e.g., ultralow absorption studies in dielectric (including solid and liquid samples), metal surfaces, and other objects which may be of physical and/or technical interest.

Last it should be noted that the technique necessary for the apparatus described above exists in the continuous band up to terahertz frequencies (*15, 16, 26–28*), which gives the possibility of broad variations of the objects studied.

V. CONCLUSION

To conclude, let us sum up the most important technical and physical results obtained in this work. A microwave resonator spectrometer having the highest sensitivity at the moment among this class of devices in the millimeter-wave band has been developed. A 90-GHz-long spectral record was obtained in one experiment, which is the broadest for such spectroscopy. The record demonstrated that a profile of the 183-GHz water line in the real atmosphere follows to the Van Vleck–Weiss-

[6] By the way, the change from amplitude to frequency measurements makes the method attractive for broad spectroscopic measurements with radiation sources which cannot continuously cover the frequency band, but rather covers it "in patches" by separate small zones of oscillation corresponding to the different modes as, e.g., in gyrotrons which reached now terahertz range (*25*), permitting the obtainment of unified absorption data independent on (different) amplitudes of oscillations at different modes.

kopf shape within 20 half-widths from the center of the line. The most accurate air-broadening parameter for this line was determined. A method of precise separate measurement of sample and resonator absorption at fixed frequency without removal of the sample from the resonator was found. With the use of this method direct measurement of atmosphere absorption at the 140 GHz "atmospheric window of transparency" was performed.

ACKNOWLEDGMENTS

The authors are thankful to Dr. P.W. Rosenkranz for providing the program for calculating the atmospheric absorption of millimeter-wave radiation and to Dr. I.N. Kozin for aid in data treatment and valuable discussions. Studies described were supported in part by RFBR grant No. 00-02-16604, joint DFG-RFBR grant No. 00-03-04001, and by state programs "Fundamental Metrology" and "Physics of the Microwaves." To all these sources of support the authors express their deep gratitude.

REFERENCES

1. C. H. Townes and A. L. Shawlow, "Microwave Spectroscopy," Dover, New York, 1975.
2. V. P. Kazakov, V. V. Parshin, and Yu. A. Dryagin, *Izv. VUZov, Radiofizika* **29,** 240–243 (1986). [in Russian; available in English as *Radiophysics and Electronics*]
3. B. S. Dumesh and L. A. Surin, *Rev. Sci. Instrum.* **67,** 3458–3464 (1996).
4. D. A. Helms and W. Gordy, *J. Mol. Spectrosc.* **66,** 206–218 (1977).
5. H. J. Liebe, P. W. Rosenkranz, and G. A. Hufford, *J. Quant. Spectrosc. Radiat. Transfer* **48,** 629–643 (1992).
6. A. Bauer, B. Duterage, and M. Godon, *J. Quant. Spectrosc. Radiat. Transfer* **36,** 307–318 (1986).
7. A. F. Krupnov, V. V. Parshin, G. Yu. Golubyatnikov, I. I. Leonov, Yu. N. Konoplev, and V. N. Markov, *IEEE Trans. Microwave Theory Tech.* **47,** 284–289 (1999).
8. A. F. Krupnov, M. Yu. Tretyakov, V. V. Parshin, V. N. Shanin, and M. I. Kirillov, *Int. J. Infrared Millimeter Waves* **20,** 1731–1737 (1999).
9. P. K. Yu and A. L. Cullen, *Proc. R. Soc. London, Ser. A* **380,** 49–71 (1982).
10. H. J. Liebe, *Radio Sci.* **20,** 1069–1089 (1985).
11. P. W. Rosenkranz, *Radio Sci.* **33,** 919–928 (1998); correction, *Radio Sci.* **34,** 1025 (1999).
12. M. Born and E. Wolf, "Principles of Optics," Pergamon Press, New York, 1968.
13. A. E. Kaplan, *Radiotechnika i Elektronika* **9,** 1781–1787 (1964). [in Russian]
14. I. S. Grigoriev and E. Z. Meilichov (Eds.), "Physical Constants," Energoatomizdat, Moscow, 1991.
15. M. B. Golant, R. L. Vilenskaya, E. A. Zyulina, Z. F. Kaplun, A. A. Negirev, V. A. Parilov, E. B. Rebrova, and V. S. Saveliev, *Pribory i Technika Eksperimenta* **4,** 136–139 (1965). [in Russian; available in English as *Sovjet Physics-Pribory*]
16. A. F. Krupnov, *Izv. VUZov, Radiofizika* **41,** 1361–1374 (1998). [in Russian: available in English as *Radiophysics and Electronics* (923–934 Engl. trans.)]; A. F. Krupnov, *Spectrochim. Acta, Part A* **52,** 967–991 (1996).
17. W. Gordy and R. L. Cook, "Microwave Molecular Spectra," Wiley–Interscience, New York, 1984.
18. H. M. Pickett, R. L. Poynter, E. A. Cohen, M. L. Delitsky, J. C. Pearson, and H. S. P. Muller, *J. Quant. Spectrosc. Radiat. Transfer* **60,** 883–890 (1998).
19. A. F. Krupnov and V. N. Markov, *Optika atmosfery i okeana* **5,** 214–215 (1992). [in Russian]
20. V. Ya. Ryadov and N. I. Furashov, *Izv. VUZov, Radiofizika* **18,** 358–369 (1975). [in Russian; available in English as *Radiophysics and Electronics*]
21. A. Bauer, M. Godon, and B. Duterage, *J. Quant. Spectrosc. Radiat. Transfer* **33,** 167–175 (1985).
22. J. R. Rusk, *J. Chem. Phys.* **42,** 493–500 (1965).
23. Yu. A. Dryagin, A. G. Kislyakov, L. M. Kukin, A. I. Naumov, and L. I. Fedoseev, *Izv. VUZov, Radiofizika* **9,** 1078–1084 (1966). [in Russian; available in English as *Radiophysics and Electronics*]
24. L. Frenkel and D. Woods, *Proc. IEEE* **54,** 498–505 (1966).
25. T. Idehara, FIR Center Report FU-2 Special, Fukui University, July 1999.
26. G. Winnewisser, A. F. Krupnov, M. Yu. Tretyakov, M. Liedtke, F. Lewen, A. H. Saleck, R. Schieder, A. P. Shkaev, and S. A. Volokhov, *J. Mol. Spectrosc.* **165,** 294–300 (1994).
27. M. Yu. Tretyakov, A. F. Krupnov, and S. A. Volokhov, *JETP Lett.* **61,** 75–77 (1995). [79–82 English translation]
28. Yu. A. Dryagin, V. V. Parshin, A. F. Krupnov, N. Gopalsami, and A. C. Raptis, *IEEE Trans. Microwave Theory Techn.* **44,** 1610–1613 (1996).